ELSEVIER

Lighting up micro-structured materials with four-wave mixing microscopy

Jordan Brocious and Eric O. Potma*

University of California, Irvine, USA

Ongoing progress in micro- and nano-material fabrication has led to novel devices and new optical properties have emerged. Among these properties are high optical nonlinearities, which can be used for light-based operations such as frequency shifting and optical computing. Optimizing and utilizing optical nonlinearities requires sensitive instruments to study them. Given the miniature sizes of the new materials under study, conventional analysis approaches may be insufficient, thus putting an emphasis on emerging technologies. Four-wave mixing (FWM) microscopy is a budding technique that is poised to become a useful tool in materials science. FWM microscopy provides a fast eye for spotting small structures and uncovering their material properties. The FWM signal derives its selectivity from material-specific electronic resonances and Raman transitions, providing an optical microscope that is attuned to visualizing and studying a broad range of micro- and nano-structured materials. In this article, the basics of FWM microscopy are discussed and the impact of this technique in materials science is highlighted.

Introduction

Smaller is better in the field of material synthesis, and progress made toward fabricating and controlling new materials on smaller and smaller scales is truly astonishing. Materials such as metals, inorganic semiconductors, organic molecules and composite compounds are crafted into diverse structures on the micro- and nanoscale from wires to quantum dots. Along with mastering the morphology of these new materials down to the nanometer scale, researchers have seen new properties emerge, not seen before in larger sized structures. In particular, the miniaturization of materials has led to interesting new optical properties that can be employed for improving the performance of a broad spectrum of optical and opto-electric devices.

The vast progress in material synthesis has also triggered a need for tools to analyze the optical characteristics of micro- and nanostructured materials. The conventional optical microscope is well suited for the task of examining novel structures on the (sub-) micrometer length scales. Using tightly focused spots, the optical microscope can bring individual structures into view, and examine their optical properties in great detail.

In addition to the well-documented linear optical properties, many nanometer scale materials display unusually strong nonlinear optical (NLO) properties. Such properties can be exploited for improving frequency shifters, nonlinear photo-detectors, and light-based computational circuits, to name just a few. Evidently, harnessing these optical nonlinearities for the next generation of optical devices requires a solid understanding of the nature and origin of the NLO response of the material. The availability of sensitive NLO microscopic probing techniques is paramount in this quest.

In a recent article in *Materials Today*, a comprehensive overview of NLO techniques useful for the study of nanomaterials was provided, which included a discussion of multi-photon fluorescence, pump-probe and coherent nonlinear microscopy methods [1]. In this contribution, we single out one of these techniques for a more in-depth discussion: four-wave mixing (FWM) microscopy.

FWM is a technique that uses three pulsed laser fields that illuminate the sample. The material then interacts with the fields and produces a new light field, which is subsequently collected by a sensitive photodetector. The technique retrieves information about electronic transitions in the material as well as chemical bond information through vibrational excitations. FWM can provide a detailed account of the lifetimes and dynamics of primary

*Corresponding author:. Potma, E.O. (epotma@uci.edu)

 1369-7021/06/$ - see front matter http://dx.doi.org/10.1016/j.mattod.2013.08.001

excitations, such as excitons and phonons, in individual particles and structures.

Because the optical nonlinearity of many nanomaterials is substantial, the corresponding FWM signals can be very strong. This enables fast imaging of multiple structures in a larger field of view, with frame rates of 1 Hz or higher. With such fast imaging rates the FWM signal itself can be conveniently used as marker for the particle's location. Therefore, nanoparticles with a strong FWM response can be used as probes, akin to the use of fluorescent probes in imaging studies. Unlike their fluorescent counterparts, however, FWM-based probes exhibit well-defined and narrow emission bands, and show negligible photobleaching. Recent work in this area has already pointed out the promise of FWM-based probes in biomedical imaging studies [1,2].

In this article, we review the impact of the FWM technique in materials science. We discuss FWM both as a characterization tool of micro- and nano-structured materials, and as an optical marker for emerging nano-sized probes. In the next sections, we first qualitatively explain the basics of FWM and then discuss several diverse materials that have been studied with the FWM technique.

FWM probes vibrational and electronic optical properties

Broadly, four-wave mixing denotes a class of optical techniques that uses three incoming laser light fields with radial frequencies ω_1, ω_2, and ω_3, to generate a fourth light field at frequency ω_4. The amplitude or intensity of this fourth field forms the FWM signal. In principle, many nonlinear optical techniques fall under this umbrella. A particular form of four-wave mixing is when the frequencies of two incoming fields are identical ($\omega_1 = \omega_3$) and when the signal frequency is detected at $\omega_4 = 2\omega_1 - \omega_2$. This dual-color approach is the most common form of FWM which has become synonymous with the term FWM itself. In the remainder of this article, we will focus exclusively on the $\omega_4 = 2\omega_1 - \omega_2$ optical FWM signal.

Why is FWM so useful for investigating materials? To appreciate the qualities of FWM spectroscopy for material research, we first list several properties of this optical probing technique:

- The FWM signal grows stronger if there are more electrons in the sample that are set in motion by the incident light fields. The more the sample structure is polarized by the joint action of the light fields, as measured by the material's nonlinear susceptibility $\chi^{(3)}$, the stronger the FWM response. Table 1 lists $\chi^{(3)}$ values for several materials. The detected FWM intensity scales as $|\chi^{(3)}|^2$.
- The FWM signal grows stronger when ω_1 and/or ω_4 are close to an electronic transition frequency in the material. At these frequencies the sample is very polarizable and thus exhibits a very high nonlinear susceptibility. We denote this condition as the one-photon electronic enhancement of the FWM signal (Fig. 1d).
- The FWM signal increases when $2\omega_1$ matches an electronic transition frequency in the sample. This condition is called the two-photon electronic enhancement of the FWM response (Fig. 1b).
- The FWM signal also increases when the difference frequency $(\omega_1 - \omega_2)$ matches a Raman transition in the material. In this limit, the FWM technique is commonly called coherent anti-Stokes Raman scattering (CARS). The two-photon, Raman allowed transitions correspond to the excitation of phonon modes or molecular vibrational modes (Fig. 1c). In some cases, electronic Raman transitions can be probed as well [3].

The fact that FWM spectroscopy is sensitive to both electronic transitions and vibrational (Raman) transitions in the sample makes this approach very versatile and attractive for examining the optical properties of a wide variety of materials. The FWM technique was first pioneered by researchers in the 1960s, shortly after the invention of the laser [4]. Since then, it has been used extensively as a tool for studying nonlinear optical properties of gases, liquids and solids alike.

FWM microscopy

The usefulness of FWM in material research is particularly evident when combined with imaging. When the probing spot is focused to sub-micrometer dimensions, the FWM technique can be used to generate high-resolution images of the material based on vibrational or electronic contrast. In this fashion, chemical heterogeneities that occur on the sub-micrometer scale in the sample can be examined in great detail. In addition, microscopic probing enables a close-up view of single nano-sized or micro-sized structures, offering opportunities for the precise characterization of individual particles that are part of a larger ensemble.

The first FWM microscope was demonstrated in 1982 [5]. It was used primarily as a CARS microscope. Subsequent developments were aimed at boosting the vibrational sensitivity of FWM microscopy, which gave rise to major improvements in terms of speed, contrast, stability and ease-of-use of the nonlinear optical microscope [6–8]. While early efforts were focused predominantly on *suppressing* the electronic FWM contrast, it was later recognized that both the vibrational and electronic FWM responses constitute

TABLE 1

Magnitude of $\chi^{(3)}$ of selected materials, given in electrostatic units (esu) and the wavelength at which the value was determined.

Material	$\chi^{(3)}$ (esu)/λ (nm)	Comments	Ref.
Water	1.3×10^{-14}/1064	Transparent material	[11]
Silica	1.4×10^{-14}/1064	Transparent material	[12]
TiO_2 (rutile)	4.0×10^{-12}/1900	Semiconductor	[13]
ZnSe	1.2×10^{-11}/1064	Semiconductor	[14]
γ-Fe_2O_3	2.1×10^{-11}/1900	Semiconductor	[15]
Si	2.5×10^{-10}/1064	Semiconductor	[16]
Ag (7 nm colloids)	2.4×10^{-9}/400	Nanometallic, plasmon	[17]
Au (5 nm film)	2.8×10^{-9}/532	Nanometallic, plasmon	[18]
Graphene	1.5×10^{-7}/~800	Zero bandgap material	[19]

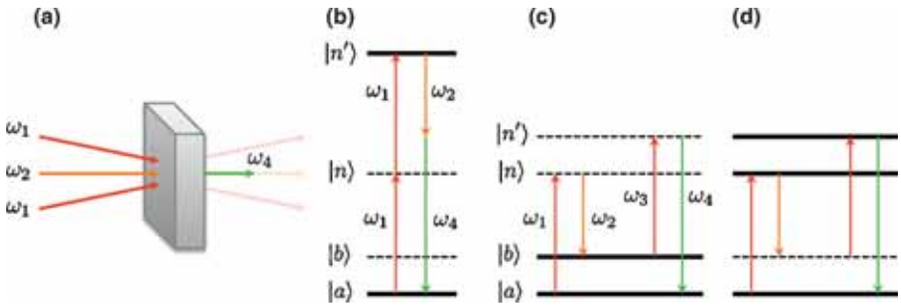

FIGURE 1

Principle of optical dual-color FWM. (a) Three light fields are incident on a sample. Two fields have optical frequency ω_1 and another has frequency ω_2. In the sample, a fourth field is generated at a new frequency $\omega_4 = 2\omega_1 - \omega_2$. (b) Two-photon enhanced electronic FWM. When the transition frequency between two electronic states in the material (solid lines) corresponds to the two-photon frequency $2\omega_1$, then the FWM signal is electronically enhanced. (c) When a vibrational transition energy in the material corresponds to the two-photon frequency $\omega_1 - \omega_2$, then the FWM is vibrationally enhanced (vibrational CARS). (d) When ω_1 or ω_4 match an electronic transition in the material, the CARS-type FWM is electronically enhanced.

useful forms of contrast for microscopic imaging of materials [2,9,10]. Some general properties of the FWM microscope are given in Table 2.

Thanks to the developments in CARS microscopy, the FWM microscope has matured into a reliable research tool. Several manufacturers offer commercial CARS microscopes that feature an intuitive user interface similar to confocal microscope systems. These user-friendly imaging platforms lend themselves very well for investigating the chemical, optical and optoelectronic properties of microstructured materials. In the following sections, we highlight several examples of applications in this area.

Structured semiconducting materials

Many semiconducting materials exhibit very high $\chi^{(3)}$ values, which is related to the presence of one-photon electronic transitions at energies that exceed the bandgap energy of the material. However, the presence of strong one-photon allowed transitions also implies that light in this energy range is linearly absorbed by the material. Many semiconducting materials are, therefore, optically nontransparent in the visible range of the spectrum. Despite the high $\chi^{(3)}$ values, the usefulness of FWM for studying semiconducting materials is then limited to examining their surfaces rather than interrogating their bulk properties. To study bulk properties, excitation energies below the bandgap energy are commonly used, where the material is optically transparent. For many semiconducting materials, this energy range lies outside the visible spectrum.

However for microstructured semiconducting materials the limited effect of attenuation combined with the high nonlinear susceptibility of the material provides favorable conditions for FWM imaging; conditions that are suitable for probing particles down to the 10 nm range. In addition, the smaller size of the material can give rise to extra effects that boost the $\chi^{(3)}$ response of the object. These effects include enhancement of the excitation field due to geometric confinement, and quantum-size effects in nanoscopic semiconducting particles.

Silicon is an excellent example of a material that can be studied with FWM. Silicon is a semiconducting material that is transparent at telecom wavelengths (1550 nm) and has already gained importance as an optical waveguide. In addition, Si has been used as a frequency conversion material through the process of FWM. Although one-photon transitions in Si are absent at telecom wavelengths, two-photon resonances contribute to a $\chi^{(3)}$ value that is still substantial, giving rise to high FWM efficiencies in the bulk material. When the excitation energies exceed the band gap, corresponding to wavelengths of ~1100 nm and below, the nonlinear susceptibility is electronically enhanced by one-photon transitions. In this regime, very strong FWM signals from nanostructured silicon are observed. The FWM signal can thus be used to study the nonlinear optical response of silicon nanoparticles [20]. Although the spatial resolution of far-field FWM microscopy is insufficient to resolve the nanometer-sized features of the particles, details down to 100 nm can be observed [21]. Some examples are shown in Fig. 2. Silicon nanowires as small as 5 nm in diameter have been shown to produce substantial FWM signals [22]. Moreover, Si nanowires were found to be very photostable with limited deterioration under regular imaging conditions. Their stability and lack of photobleaching suggest that Si nanowires can be used as durable FWM-based probes for biomedical imaging applications [22].

TABLE 2

Selected properties of the FWM microscope.

Property	Specification	Comments
Lateral resolution	0.3 μm	Dependent on wavelength and objective lens. Higher resolution is possible.
Axial resolution	~1.0 μm	
Contrast	Electronic transitions Vibrational transitions	Materials that exhibit strong one-photon or two-photon absorption bands generally have strong FWM signals. Vibrational contrast arises from modes with strong Raman scattering cross sections.
Pixel dwell time	~0.1 μs	Supports video-rate scanning with a 512 × 512 frame size.
Sensitivity	Single nanostructures	Structures down to 5 nm can be individually probed, depending on the $\chi^{(3)}$ of the material.
Concentration scaling	N^2	N is the number density of dipolar contributors to the signal. When phase sensitive detection is used, the signal scales as N.

Binary semiconducting metal oxide nanostructures have also been successfully visualized in the FWM microscope. Compared to silicon, many metal oxides have higher bandgap energies and display transparency at near-infrared wavelengths. At near-infrared excitation wavelengths, away from one-photon electronic resonances, the nonlinear susceptibility of many metal oxides is significantly lower than that of silicon. However, the NLO response of metal oxide nanoparticles is still considerable, producing bright FWM signals that are much stronger than the FWM background from biological tissues. Titanium dioxide [23,24], cerium oxide [24], zinc oxide [24,25] and iron oxide [26,27] nanoparticles have been used as NLO probes in tissues and cells.

FWM has also been instrumental in the study of the excitation dynamics in semiconducting GaAs and PbS quantum dots [28–30]. Time-resolved experiments on individual dots have provided important information about particle-specific dephasing of excitons in these materials. Moreover, the strong $\chi^{(3)}$ response of binary semiconducting materials has been used in imaging applications, such as the use of CdSe/ZnS quantum dots as FWM labels in cellular imaging studies [31].

Structured metals

Although elemental metals have high nonlinear susceptibility values, the non-propagating character of light in metals limits the generation of FWM signals to those parts of the material that fall within the skin depth, amounting to only fraction of an optical wavelength from the surface. Consequently, experiments aimed at studying the nonlinear optical properties of bulk metals are typically carried out in reflection mode.

However, the situation for nanosized metal objects is different. First, because the size of the particle is on the order of the skin depth or less, the entire structure contributes to the FWM signal. Second, for a variety of metals the third-order optical response is enhanced by the presence of extra resonances in the particle due to collective motions of surface electrons. These resonances are called surface plasmon resonances. Depending on the size and shape of the structure, and the dielectric properties of the material, the frequency of the surface plasmon resonances can appear in the visible range of the spectrum. Particles in the 10–100 nm range of gold or silver fall into this category. The presence of surface plasmon modes condenses the energy of the electric field to a very small region near the metal surface, thereby enhancing the amplitude of the field locally. These very strong local electric fields dramatically alter the nonlinear response of the metal particle in two ways: (a) the strong surface field *inside* the metal enhances the FWM response of the material itself, and (b) the strong surface field *outside* the metal can boost the FWM signal from other compounds in close proximity of the metal surface.

The magnitude of the surface plasmon enhanced FWM signal of gold and silver nanoparticles is significant, and the signal can be easily detected in the nonlinear FWM microscope. This principle was demonstrated in as early as 1983 [32], and has since been used to examine the optical coupling between proximal nanospheres [33] and the nature of the nonlinear optical response of individual metal nanostructures [34–38]. The FWM from nanogold structures has also been used in cell and tissue imaging studies, where the nanoparticles can be used as functionalized probes [39–43]. The ease of synthesizing gold and silver nanoparticles, and the progress made in chemically functionalizing them, suggests that these materials are promising candidates for NLO probes in biomedicine. However, their utility is ultimately determined by the degree of phototoxicity associated with metal nanoparticles, which is currently not fully understood. Beyond metal nanoparticles, FWM microscopy has also been used to generate nonlinear signals from flat metal surfaces. For these materials, the surface excitations are different: they are non-local and described as propagating surface plasmons polaritons (SPP). FWM with SPP modes have led to the observation of new and interesting nonlinear optical phenomena at metal surfaces [44–48].

When the surface field outside the particle is used for enhancing the response of molecules close to the metal nanoparticle, otherwise weak FWM signals from molecular compounds can be significantly amplified. This principle has been used in vibrationally sensitive, surface-enhanced (SE-)CARS microscopy, which can be considered as a nonlinear analog of surface enhanced Raman scattering (SERS). SE-CARS was first demonstrated on flat silver films [49] and is currently used to enhance the nonlinear Raman response from molecules tethered to colloidal nanometals [50–53] or patterned nanostructures [54].

Nanostructured carbon materials

Graphene consists of single planar sheets of sp^2 hybridized carbon atoms, and is considered a zero-gap semiconductor in which interband one-photon transitions are allowed for all photon energies. Graphene is thus a 'maximally resonant' material, as all possible one-photon and multi-photon resonances contribute to the third-order optical signal. Consequently, graphene exhibits an exceptionally large value for the nonlinear susceptibility, which ranks its optical nonlinearity among the highest of all solid state materials. The high $\chi^{(3)}$ response of the material makes it possible to generate bright FWM signals from single sheets of graphene in an optical microscope [19]. FWM experiments provide important clues toward understanding the nature of the excitation dynamics in graphene [55–57]. Moreover, the graphene FWM signal is stable, resistant to photodamage, and virtually independent of the input wavelengths. These qualities render graphene an ideal material for FWM frequency shifting applications [58–60].

The structure of carbon nanotubes is derived from graphene, equivalent to rolling graphene sheets into tubes with nanoscopic diameters. Tubes can be formed by rolling graphene at different pitch angles, giving rise to a wide variety of carbon nanotube chiralities, each with their own characteristic electronic band structure. Compared to graphene, the quasi one-dimensional character of the nanotubes produces more discrete distributions of states within the band structure of the material, which give rise to specific optical resonances. Based on the different electronic bandstructures of carbon nanotubes these materials can be divided into two classes: semiconducting and metallic nanotubes. The optical response of carbon nanotubes in the visible range of the spectrum is characterized by electronic inter- and intra-band transitions. This yields a high nonlinear susceptibility for carbon nanotubes, which is many orders of magnitude larger compared to the $\chi^{(3)}$ of common dielectric materials [61,62]. FWM spectroscopy has been used extensively to study the phonon dynamics in carbon nanotubes, both in bulk samples [63,64] as well as in microscopic bundles of nanotubes [65]. Using tip-enhanced CARS

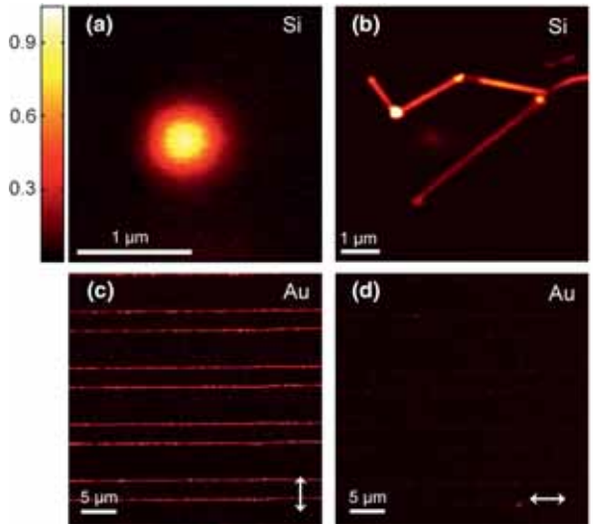

FIGURE 2

FWM of elemental materials. (a) Silicon nanoparticles (30 nm width) produce very strong FWM signals. (b) Silicon nanowires (100 nm width) visualized with ~150 nm super-resolution FWM. Adapted and reprinted with permission from Ref. [21]. (c) Strong FWM signals from gold nanowires (20 nm high, 186 nm wide) are seen when the polarization of the incident light (arrow) is aligned with a surface plasmon mode of the wire. (d) Dimmer FWM signals are seen when the polarization of the light is perpendicular to the orientation of the plasmon mode.

microscopy, individual carbon nanotubes were recently visualized based on contrast derived from the bond vibrations of the carbon skeleton [66]. In addition, the purely electronic FWN signal can be used to map individual nanotubes [67] and measure their electronic dephasing times [68]. The electronic FWM was shown to be sensitive to the density of charge carriers, providing a good probe for monitoring local electric and chemical changes in individual carbon nanotubes (Fig. 3) [3].

Micro- and nano-structured polymer materials

Compared to solid inorganic compounds, the nonlinear susceptibility of many polymers is much lower. However, the delocalized electrons in the backbone of conjugated polymers can raise the electronic polarizability of these molecular systems to appreciable levels. Similarly, highly polarizable chemical side groups give the nonlinear susceptibility of certain polymers a boost. Consequently, the FWM signals of a wide variety of polymers are strong enough for fast imaging applications.

In particular, the vibrational FWM response of polymers provides rich information about the material. For instance, the CARS signal from skeletal C–C vibrations is suitable for rapidly mapping out polymer photoresists, enabling a quick inspection of the chemical changes on a microscopic scale imprinted after patterned UV illumination [69]. Similarly, CARS microscopy is a good choice for visualizing microscopic segregated domains in mixtures of different polymers. Using multiplex CARS microscopy, which derives contrast from multiple vibrational bands simultaneously, the different domains can be identified based on subtle chemical differences between the polymer ingredients in the blend [70–73]. In addition, this approach is useful for studying the quality of layered polymer films, as the different layers can be inspected *in situ* without the use of labels [74,75]. Note that the vibrational FWM signal is accompanied by an electronic FWM response of the material. These two components mutually interfere, which gives rise to vibrational CARS spectra that appear differently shaped compared to conventional Raman spectra. The distorted line shape in CARS microspectroscopy is sometimes perceived as an analytical disadvantage compared to linear Raman spectroscopy. Nonetheless, recently developed phase retrieval algorithms make it possible to convert CARS spectra to the corresponding Raman spectra [76,77], allowing researchers to take full advantage of the fast imaging properties of FWM microscopy while retaining Raman analytical capabilities.

The chemical selectivity of Raman sensitive FWM is also useful in monitoring the formation of polymer structures through multiphoton induced polymerization, a fabrication method for polymer microstructures based on principles similar to 3D laser writing. CARS microscopy is capable of seeing the chemical differences induced by the writing process, thus enabling a close up view of the chemical and morphological qualities of the structure while it is being written [78,79].

Furthermore, the fast imaging capabilities of vibrationally sensitive FWM make it possible to follow the release of particular drugs such as paclitaxel from polymer hosts [80–82]. The ability to image the changes on a microscopic scale to both the drugs as well as the polymer matrix during the release process has unraveled aspects of the dissolution dynamics that have previously gone unnoticed. FWM microscopy can also play a role in drug release studies from smaller sized polymer delivery systems, such as poly(lactic-co-glycolic acid) (PGLA) nanoparticles. Such systems have attracted attention as delivery vehicles for various drugs to targeted parts of the body. The success of such drug carriers depends on the uptake and subsequent release of the particles by cells and tissues. FWM imaging has enabled the visualization of

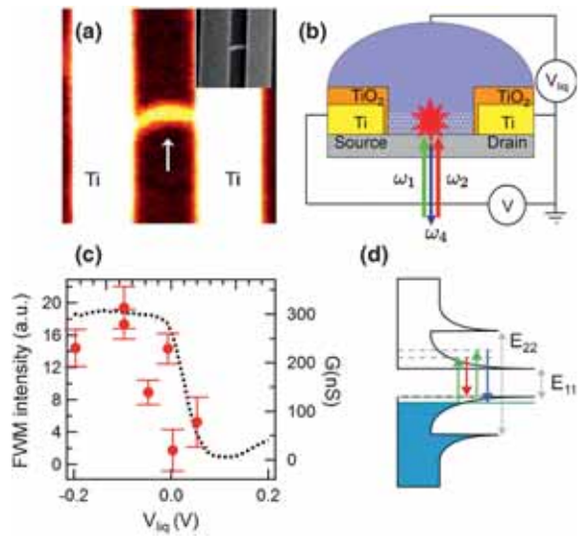

FIGURE 3

FWM of carbon nanotubes. (a) FWM image of a carbon nanotube (arrow) between two Ti electrodes. The inset shows the scanning electron micrograph (SEM). (b) Schematic of liquid gating experiments on a carbon nanotube. (c) Change of the FWM signal (red dots) and conductance G (dashed line) as a function of the gating voltage V_{liq} for a semiconducting carbon nanotube. The FWM signal tracks the conductance of the nanotube. (d) All-electronic CARS process that accounts for the conductance dependence of the FWM signal. Based on data discussed in Ref. [3].

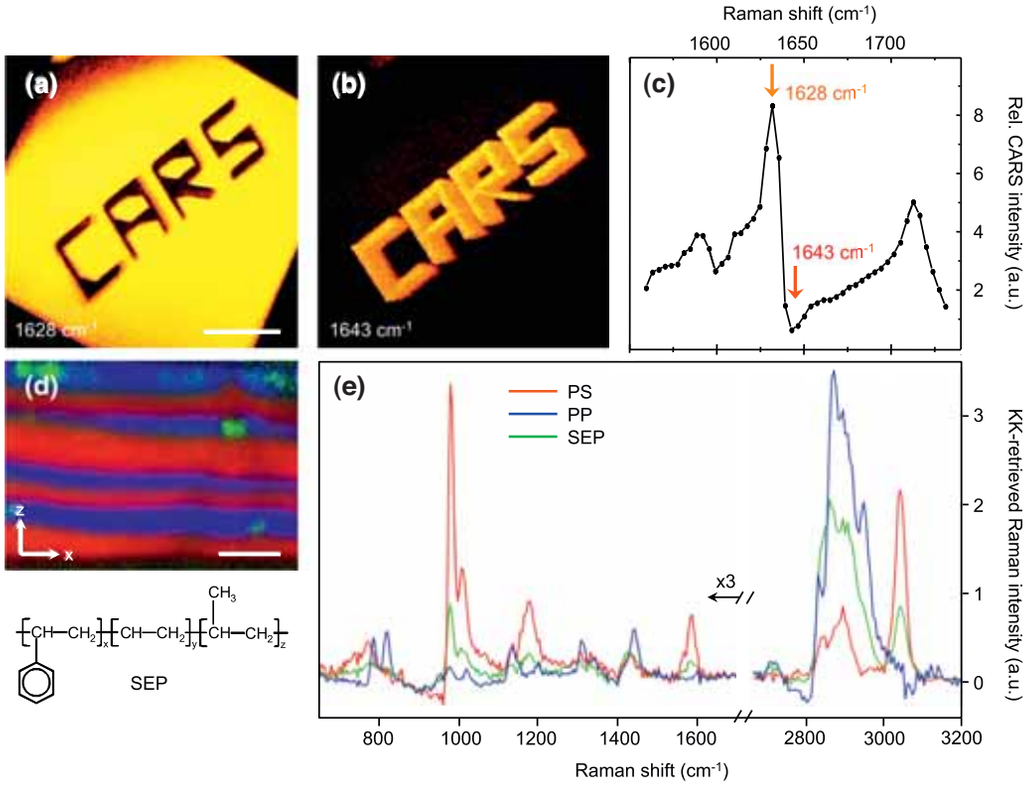

FIGURE 4

FWM of polymer materials. (a) 3D rendering of a CARS image of a polymer structure written with two-photon induced polymerization of acrylic monomers. At the vibrational frequency of 1628 cm^{-1}, the carbonyl bond of the monomer is resonant, highlighting the non-polymerized solution. (b) Same structure visualized at 1648 cm^{-1}, where the signal of the monomer is minimal, effectively highlighting the polymerized structure. Scale bar is 20 μm. (c) CARS vibrational spectrum of the monomer. Panels (a–c) are based on data discussed in Ref. [79]. (d) Layered polymer sample of polystyrene (PS; red), polypropylene (PP; blue) and a poly(styrene-ethylene/propylene) diblock co-polymer (SEP; green). Note that the polymers can be discriminated based on differences in the Raman spectra. Scale bar is 20 μm. (e) Raman spectra of the three different polymers, as retrieved from the CARS spectra using the modified Kramers–Kronig (KK) phase retrieval method. Adapted and reprinted with permission from Ref. [74], copyright 2011 American Chemical Society.

the distribution of biocompatible polymer nanoparticles in cells and tissues [83,84], information crucial for the further development of these drug delivery systems (Fig. 4).

Organic microcrystallites

Densely packed organic molecules, such as found in microcrystallites, exhibit high numbers of chemical bonds per unit volume. At these densities, vibrational FWM signals can be sizable, permitting fast imaging of crystallized organic molecules. This capability aids in identifying and examining bioorganic microcrystallites. For example, CARS has helped with the chemically selective detection of spontaneously formed crystals of cholesterol monohydrate and cholesteryl esters in atherosclerotic lesions [85]. The aligned molecules in the crystal give rise to a polarization sensitive FWM signal, which allows detailed investigations of the orientation and order of the microcrystallites. This principle has been used for generating detailed maps of the orientation of organic microcrystals, as shown in Fig. 5.

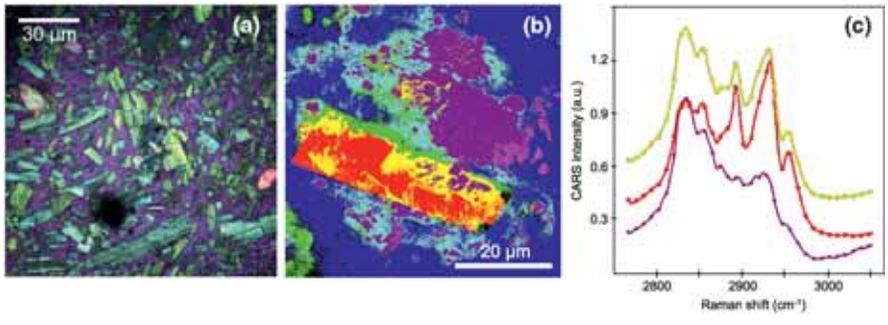

FIGURE 5

FWM microscopy of (bio-)organic microcrystallites. (a) Solid dosage form composed of diprophylline (lime green and teal), tristearin (magenta) and mannitol (pale yellow and pink). Different colors are based on differences in the CARS spectra, defined by the chemical structure and the orientation of the microcrystallite. Courtesy of Erik Garbacik and Herman Offerhaus, Twente University, the Netherlands. (b) False color map based on a hyperspectral CARS image of an atherosclerotic plaque. The CARS spectra corresponding to the yellow, red and purple pixels are given in panel (c). The red spectrum matches the spectrum of crystalline cholesterol monohydrate, indicating that microcrystallites of cholesterol can be found in the plaque. Panels (b,c) are based on data discussed in Ref. [85].

The chemically selective imaging capability is also helpful in analyzing several preparations of pharmaceutical specimens [86]. An example includes the ability to monitor the release of drugs from tablets. For this purpose, CARS microscopy has been used to bring into view the chemical and structural properties of the tablet material [87,88]. The success of these studies insinuates that the vibrational FWM technique may play an important role in elucidating the homogeneity, size distribution, dissolution efficacy and spontaneous phase transformations of the tablet materials during storage.

The electronic FWM contrast has also been used in studying organic microcrystallites. For many elongated organic compounds packed into microscopic domains, the electronic signal is highly dependent on molecular orientation. This feature has been exploited, for instance, in the study of liquid crystals. Using both electronic and vibrational signatures, FWM microscopy has been used to visualize the re-orienting response of microdomains to external electric cues [89,90].

Conclusion

FWM microscopy has been used primarily for biological imaging, and its application to materials science is relatively new. However, the above examples demonstrate that the FWM technique is a versatile research tool in the study of micro- and nano-sized materials. The combination of the high spatial resolution, the fast signal acquisition and the electronic and vibrational sensitivity make FWM a highly attractive label-free and nondestructive method both for studying the optical properties of materials as well as for imaging the spatial distribution of new materials with microscopic precision. The clear advantages of FWM microscopy as a research tool continue to translate into a growing number of applications and publications in the area of materials science.

Acknowledgments

We thank financial support from the Department of Energy, Office of Research, Basic Energy Sciences, Grant DE-SC0003905, and from the National Science Foundation, Center for Chemical Innovation, Grant CHE-0802913.

References

[1] L. Tong, J.X. Cheng, Mater. Today 14 (6) (2011) 264–273.
[2] Y. Wang, et al. Adv. Opt. Photon. 3 (1) (2011) 1–52.
[3] T. Sheps, et al. Phys. Rev. B 86 (23) (2012) 235412.
[4] P.D. Maker, R.W. Terhune, Phys. Rev. 137 (3A) (1965) A801–A818.
[5] M.D. Duncan, J. Reintjes, T.J. Manuccia, Opt. Lett. 7 (8) (1982) 350–352.
[6] A. Zumbusch, G.R. Holtom, X.S. Xie, Phys. Rev. Lett. 82 (20) (1999) 4142–4145.
[7] J.-X. Cheng, X.S. Xie, J. Phys. Chem. B 108 (3) (2003) 827–840.
[8] J.X. Cheng, X.S. Xie, Coherent Raman Scattering Microscopy, CRC Press, Boca Raton, 2013.
[9] K. Isobe, et al. Appl. Phys. Express 1 (2008) 022006.
[10] D. Akimov, et al. J. Raman Spectrosc. 40 (8) (2009) 941–947.
[11] D. Débarre, E. Beaurepaire, Biophys. J. 92 (2) (2007) 603–612.
[12] U. Gubler, C. Bosshard, Phys. Rev. B 61 (16) (2000) 10702–10710.
[13] T. Hashimoto, T. Yoko, S. Sakka, Bull. Chem. Soc. Jpn. 67 (3) (1994) 653–660.
[14] S. Adachi, Properties of Group IV, II-V and II-VI Semiconductors, John Wiley & Sons, Ltd., Chichester, 2005.
[15] T. Hashimoto, T. Yamada, T. Yoko, J. Appl. Phys. 80 (6) (1996) 3184–3190.
[16] L.I. Berger, in: D.R. Lide (Ed.), CRC Handbook of Chemistry and Physics, 90th ed., Taylor & Francis, Boca Raton, 2009.
[17] D. Ricard, P. Roussignol, C. Flytzanis, Opt. Lett. 10 (10) (1985) 511–513.
[18] E. Xenogiannopoulou, et al. Opt. Commun. 275 (1) (2007) 217–222.
[19] E. Hendry, et al. Phys. Rev. Lett. 105 (9) (2010) 097401.
[20] V. Raghunathan, E.O. Potma, J. Opt. Soc. Am. A 27 (11) (2010) 2365–2374.
[21] H. Kim, G.W. Bryant, S.J. Stranick, Opt. Express 20 (6) (2012) 6042–6051.
[22] Y. Jung, et al. Nano Lett. 9 (6) (2009) 2440–2444.
[23] H. Chen, et al. Opt. Express 17 (3) (2009) 1282–1290.
[24] J. Moger, B.D. Johnston, C.R. Tyler, Opt. Express 16 (5) (2008) 3408–3419.
[25] A.V. Kachynski, et al. J. Phys. Chem. C 112 (29) (2008) 10721–10724.
[26] Y. Zheng, G. Holtom, S. Colson, Proc. SPIE 5323 (2004) 390–399.
[27] G. Rago, et al. Biomed. Opt. Express 2 (9) (2011) 2470–2483.
[28] N.H. Bonadeo, et al. Phys. Rev. Lett. 81 (13) (1998) 2759–2762.
[29] F. Masia, et al. Phys. Rev. B 82 (15) (2010) 155302.
[30] F. Masia, et al. Phys. Rev. B 83 (20) (2011) 201309.
[31] F. Masia, W. Langbein, P. Borri, Appl. Phys. Lett. 93 (2) (2008), 021114-021114-3.
[32] D.S. Chemla, et al. Phys. Rev. B 27 (8) (1983) 4553–4558.
[33] M. Danckwerts, L. Novotny, Phys. Rev. Lett. 98 (2) (2007) 026104.
[34] P. Stefano, D. Matthias, N. Lukas, J. Opt. A: Pure Appl. Opt. 11 (11) (2009) 114030.
[35] K. Hyunmin, et al. Nano Lett. 8 (8) (2008) 2373–2377.
[36] P. Sasanpour, A. Shahmansouri, B. Rashidian, J. Nanosci. Nanotechnol. 10 (11) (2010) 7179–7182.
[37] F. Masia, W. Langbein, P. Borri, Phys. Rev. B 85 (23) (2012) 235403.
[38] P. Genevet, et al. Nano Lett. 10 (12) (2010) 4880–4883.
[39] Y. Jung, et al. J. Phys. Chem. C 113 (7) (2009) 2657–2663.
[40] F. Masia, et al. Opt. Lett. 34 (12) (2009) 1816–1818.
[41] N. Garrett, M. Whiteman, J. Moger, Opt. Express 19 (18) (2011) 17563–17574.
[42] Y.-S. Chen, et al. Nanoscale Res. Lett. 4 (8) (2009) 858–864.
[43] G. Rago, et al. J. Phys. Chem. B 115 (17) (2011) 5008–5016.
[44] S. Palomba, L. Novotny, Phys. Rev. Lett. 101 (5) (2008) 056802.
[45] J. Renger, et al. Phys. Rev. Lett. 103 (26) (2009) 266802.
[46] J. Renger, et al. Phys. Rev. Lett. 104 (4) (2010) 046803.
[47] X. Liu, Y. Wang, E.O. Potma, Opt. Lett. 36 (12) (2011) 2348–2350.
[48] S. Palomba, et al. Nat. Mater. 11 (2012) 34–38.
[49] C.K. Chen, et al. Phys. Rev. Lett. 43 (13) (1979) 946–949.
[50] T.-W. Koo, S. Chan, A.A. Berlin, Opt. Lett. 30 (9) (2005) 1024–1026.
[51] T. Ichimura, et al. J. Raman Spectrosc. 34 (9) (2003) 651–654.
[52] C. Steuwe, et al. Nano Lett. 11 (12) (2011) 5339–5343.
[53] V. Namboodiri, et al. Vib. Spectrosc. 56 (1) (2011) 9–12.
[54] C. Steuwe, et al. Proc. SPIE: Int. Soc. Opt. Eng. 8234 (2012), 82340E (7 pp.).
[55] K. Kang, et al. Phys. Rev. B 81 (16) (2010) 165405.
[56] Z.B. Liu, et al. Chin. Sci. Bull. 57 (23) (2012) 2971–2982.
[57] Z.S. Zhang, P.L. Voss, Opt. Lett. 36 (23) (2011) 4569–4571.
[58] Z.Q. Luo, et al. J. Lightwave Technol. 29 (18) (2011) 2732–2739.
[59] B. Xu, A. Martinez, S. Yamashita, IEEE Photon. Technol. Lett. 24 (20) (2012) 1792–1794.
[60] T. Gu, et al. Nat. Photon. 6 (8) (2012) 554–559.
[61] D. Shimamoto, et al. Appl. Phys. Lett. 92 (8) (2008) 081902.
[62] W. Zhao, J. Phys. Chem. Lett. 2 (5) (2011) 482–487.
[63] K. Ikeda, K. Uosaki, Nano Lett. 9 (4) (2009) 1378–1381.
[64] V.A. Margulis, O.V. Boyarkina, E.A. Gaiduk, Opt. Commun. 249 (1–3) (2005) 339–349.
[65] A.S. Duarte, et al. Nano Lett. 13 (2) (2013) 697–702.
[66] K. Furusawa, et al. J. Raman Spectrosc. 43 (5) (2012) 656–661.
[67] H. Kim, et al. Nano Lett. 9 (8) (2009) 2991–2995.
[68] P. Myllyperkio, et al. ACS Nano 4 (11) (2010) 6780–6786.
[69] E.O. Potma, et al. J. Phys. Chem. B 108 (4) (2003) 1296–1301.
[70] T.W. Kee, M.T. Cicerone, Opt. Lett. 29 (23) (2004) 2701–2703.
[71] Y.J. Lee, et al. ACS Macro Lett. 1 (11) (2012) 1347–1351.
[72] S.-H. Lim, et al. J. Phys. Chem. B 110 (11) (2006) 5196–5204.
[73] B. von Vacano, L. Meyer, M. Motzkus, J. Raman Spectrosc. 38 (7) (2007) 916–926.
[74] Y.J. Lee, et al. Anal. Chem. 83 (7) (2011) 2733–2739.
[75] J.S. Yahng, S.C. Jeoung, Opt. Lasers Eng. 49 (1) (2011) 66–70.
[76] E.M. Vartiainen, et al. Opt. Express 14 (2006) 3622–3630.
[77] Y. Liu, Y.J. Lee, M.T. Cicerone, Opt. Lett. 34 (9) (2009) 1363–1365.
[78] T. Baldacchini, R. Zadoyan, Opt. Express 18 (18) (2010) 19219–19231.
[79] T. Baldacchini, et al. J. Phys. Chem. B 113 (38) (2009) 12663–12668.
[80] E. Kang, et al. J. Control. Rel. 122 (3) (2007) 261–268.
[81] E. Kang, et al. Anal. Chem. 78 (23) (2006) 8036–8043.
[82] E. Kang, et al. J. Biomed. Mater. Res. A 87A (4) (2008) 913–920.
[83] P.S. Xu, et al. Mol. Pharm. 6 (1) (2009) 190–201.
[84] N.L. Garrett, et al. J. Raman Spectrosc. 43 (5) (2012) 681–688.
[85] R.S. Lim, et al. J. Lipid Res. 52 (2011) 2177–2186.
[86] C.J. Strachan, M. Windbergs, H.L. Offerhaus, Int. J. Pharm. 417 (1/2) (2011) 163–172.
[87] M.N. Slipchenko, et al. Analyst 135 (10) (2010) 2613–2619.
[88] M. Windbergs, et al. Anal. Chem. 81 (6) (2009) 2085–2091.
[89] B.C. Chen, S.H. Lim, Appl. Phys. Lett. 94 (17) (2009) 171911.
[90] B.G. Saar, et al. Opt. Express 15 (21) (2007) 13585–13596.